

Transition between Flux Liquid and Flux Solid in High- T_c Superconductors

Lei Xing⁽¹⁾ and Zlatko Tešanović^{(1),(2)}

⁽¹⁾*Department of Physics and Astronomy, Johns Hopkins University, 3400 North Charles Street, Baltimore, Maryland 21218*

⁽²⁾*Theoretical Division, MS B262, Los Alamos National Laboratory, Los Alamos, New Mexico 87545*
(Received 8 March 1990)

We have studied flux melting near the H_{c1} line in Y-Ba-Cu-O using a variational Monte Carlo method. The existence of a flux-liquid phase has been observed and the transition line between flux liquid and flux solid in the H - T phase diagram has been determined. The width of the liquid phase increases with temperature as T^2 at low temperatures, as predicted by Nelson, and faster than T^2 at higher temperatures, eventually crossing over to the high-field melting curve.

PACS numbers: 74.60.Ge

One of the most interesting properties of the high- T_c superconducting oxides is the unconventional behavior of the flux-line lattice (FLL). In ordinary, "low- T_c ," bulk type-II superconductors, the Abrikosov FLL is essentially stable throughout the mixed-phase portion of the phase diagram in the H - T plane (only when the external field H is very close to the mean-field H_{c2} will the thermal fluctuations start affecting the positional order). The FLL of the new oxide superconductors is, however, melted well below the mean-field value of H_{c2} [$T_c(H)$],¹⁻⁵ similar to what is expected in two-dimensional thin films.⁶ Moreover, recent experiments indicate that in a single crystal of $\text{YBa}_2\text{Cu}_3\text{O}_{7-x}$ there exist two distinct vortex-liquid regimes, a hexaticlike region followed by an entangled isotropic region.^{7,8} This novel phenomenon of a flux lattice melting is directly related to the weak interplanar couplings, small intrinsic intraplane coherence length, and high critical temperatures in copper-oxide superconductors.

One can study statistical mechanics of the FLL by mapping flux lines onto a two-dimensional interacting quantum system.² This mapping, in which we assume, for simplicity, that the interaction is instantaneous and neglect the directional dependence of the electromagnetic vortex interaction,⁹ predicts that a flux liquid will always exist at any finite temperature at fields slightly higher than the lower critical field H_{c1} . By arguing that the ground state is a superfluid entangled vortex liquid and using the results for a 2D hard-disk boson system,¹⁰ the transition between the flux liquid and the flux solid is given by²

$$\delta h \equiv \frac{H_x - H_{c1}}{H_{c1}} \approx \text{const} \times \left(\frac{k_B T}{\lambda \epsilon_1} \right)^2 \frac{M_z}{M}, \quad (1)$$

where $H_x(T)$ is the transition (melting) field, ϵ_1 is the energy per unit length of a single flux line, M_z is the quasiparticle effective mass along the c axis, and M is the intraplane effective mass.

In this paper we present the results of a variational Monte Carlo calculation on the flux-line system in

$\text{YBa}_2\text{Cu}_3\text{O}_{7-x}$, obtained by utilizing the mapping to the interacting quantum system. We have observed a narrow flux-liquid phase in the vicinity of H_{c1} , and determined the melting line $H_x(T)$. The "width" of the liquid phase region increases as T^2 at low temperatures, and faster than T^2 at higher temperatures, signaling the eventual crossover to the high-field melting curve determined via Lindemann's rule.⁵ We consider only the perpendicular ($\mathbf{H} \parallel c$ axis) external field which we choose to be along the z direction. In the London limit, the trajectories of vortices are isomorphic to the world lines of quantum particles (flux bosons).² Strictly speaking, these particles are not bosons and their Hilbert space is not limited to regions of specific permutation symmetry. However, if one considers an infinite superconductor, corresponding to a quantum system at $T=0$, we are only concerned with the ground state which is, quite generally, a fully symmetric wave function. Thus, for our purposes it is perfectly accurate to treat these particles as bosons. The "Hamiltonian" for the corresponding two-dimensional interacting boson system is given by

$$H = - \sum_i \frac{(k_B T)^2}{2\tilde{\epsilon}_1} \nabla_i^2 + \sum_{i < j} \frac{\phi_0^2}{8\pi^2 \lambda^2} K_0(r_{ij}/\lambda), \quad (2)$$

where $\tilde{\epsilon}_1 = (M_z/M)\epsilon_1$ and $K_0(x)$ is the modified Bessel function. Thus the problem of the flux-lattice melting can be treated as the fluid to solid phase transition in the 2D bosonic system described by the above Hamiltonian.

The nature of the bosonic ground state of the Hamiltonian (2) can be studied by a variational Monte Carlo technique. We start by choosing a Jastrow-type variational wave function that describes the ground state of the fluid phase,

$$\Psi = \prod_{i < j} f(r_{ij}) = \prod_{i < j} \exp \left[- \left(\frac{a_{10}}{\sqrt{\rho}} \frac{1}{r} \right)^{a_2} \right], \quad (3)$$

where ρ is the density and a_{10} and a_2 are two variational parameters to be determined by minimizing the Gibbs free energy for a given \mathbf{H} . In the region of flux-liquid to

flux-solid transition, we find $a_2=3$ optimizes the energy.¹¹ It is reasonable to assume that the main effect of the varying external field on the wave function is to properly rescale the density. Thus, we explicitly include the density in Eq. (3). The parameter a_{10} is then regarded as a slow varying function of the external field. The crystalline ground state was constructed by multiplying the Jastrow wave function (3) by Gaussian factors $\prod_i \exp[-A\rho(\mathbf{r}_i - \mathbf{R}_i)^2]$ centered at triangular lattice sites $\{\mathbf{R}_i\}$. These factors explicitly break the translational symmetry of the Jastrow wave function and localize

particles on lattice sites. The lack of symmetry with respect to particle interchange should not be a major shortcoming since many physical properties are quite insensitive to symmetrization.^{12,13} In the following, we compute and compare the Gibbs free energies for two phases. The transition between these two states occurs when the free energies are equal. We took the mass ratio $\sqrt{M_z/M} = 5$ deduced from the ratio of the slopes of $H_{c2\parallel}$ and $H_{c2\perp}$ and $\kappa = \lambda/\xi = 50$.⁵ The magnetic penetration depth $\lambda(T)$ is from Ref. 14.

The Helmholtz free energy per unit volume at density ρ for both liquid and solid state is obtained from

$$F = \frac{\langle \Psi | H | \Psi \rangle}{\Omega \langle \Psi | \Psi \rangle} = -\frac{\rho^2}{2} \frac{(k_B T)^2}{2\bar{\epsilon}} \int g(r) \nabla^2 \ln f(r) d\mathbf{r} + 3A\rho \frac{(k_B T)^2}{2\bar{\epsilon}} + \rho^2 \left(\frac{\phi_0}{4\pi\lambda} \right)^2 \int g(r) K_0(r/\lambda) d\mathbf{r}, \quad (4)$$

where Ω is the area and $g(r)$ is the pair-correlation function. Note that $A=0$ corresponds to a Jastrow liquid state. We can calculate F if we know the pair-correlation function $g(r)$:

$$g(r) \equiv \frac{N(N-1) \int \cdots \int |\Psi|^2 d\mathbf{r}_3 d\mathbf{r}_4 \cdots d\mathbf{r}_N}{\rho^2 \int |\Psi|^2 d\mathbf{r}_1 \cdots d\mathbf{r}_N}. \quad (5)$$

For a crystalline state, the $g(r)$ used in Eq. (4) is an average over the orientation and different lattice sites.¹² The formal analogy with a classical N -body system suggests use of the Monte Carlo method, in which sample configurations are generated from the trial wave function by the Metropolis random-walk algorithm, to calculate $g(r)$.^{15,16} The melting line in the H - T phase diagram can be found using the following approach. To begin with, we compute F using Eq. (4) for a range of densities (determined by $B!$). The external magnetic field H and the Gibbs free energy G are then found from relations $B = \rho\phi_0$, $H - H_{c1} = 4\pi\partial F/\partial B$, and $G = F - (B/4\pi)(H - H_{c1})$. The value of a_{10} had to be optimized for each B or external field H . It is important to note that the energy scaling used in the isotopes of helium is not valid any more because of the Bessel-function-type interaction potential between flux bosons.¹⁷ However, the pair-correlation function still possesses a scaling law $g_{\rho_2}(r) = g_{\rho_1}(\sqrt{\rho_1/\rho_2}r)$, where $g_{\rho_1}(r)$ and $g_{\rho_2}(r)$ are the pair-correlation functions at two different densities, ρ_1 and ρ_2 . Consequently, it is possible to use the scaled pair-correlation function $g_{\rho_2}(r)$ from a fixed density ρ_1 to perform integrals in Eq. (3) and obtain F at density ρ_2 .

All the computations were performed on the ARDENT-Titan 3 minisupercomputer. We used a 224-particle system in a rectangular box of aspect ratio $4\sqrt{3}/7$, chosen to accommodate a perfect triangular lattice at high densities. Starting from a random configuration for the liquid state and a triangular lattice for the crystalline state, we let the system approach equilibrium for 336 000 steps and took the average over the next 873 600 steps. The size-dependent effects were found to be negligible. The overall statistical error is es-

timated to be less than 4% on the Gibbs free energy G . The extensive running time made it impractical to exactly optimize the wave function for each external field. These uncertainties would decrease for higher densities. In Fig. 1 we have plotted the Gibbs free energy versus external field in the region of the phase transition at $T=10.58$ K. The main feature is that, for $H - H_{c1}$ higher than 0.71×10^{-7} Oe, the optimum value $A \neq 0$, whereas for $H - H_{c1}$ lower than 0.71×10^{-7} Oe it is the value $A = 0$ that yields the minimum energy, indicating that the system prefers a fluid-type state to a solid-type one. The corresponding transition densities are $\rho_{\text{fluid}} = 2.60 \times 10^6 \text{ cm}^{-2}$ and $\rho_{\text{solid}} = 2.73 \times 10^6 \text{ cm}^{-2}$, or $7.56 \times 10^{-4} (\lambda^{-2})$ and $7.93 \times 10^{-4} (\lambda^{-2})$ in terms of reduced units, respectively. The kinetic energy is about an order of magnitude larger than the potential energy at

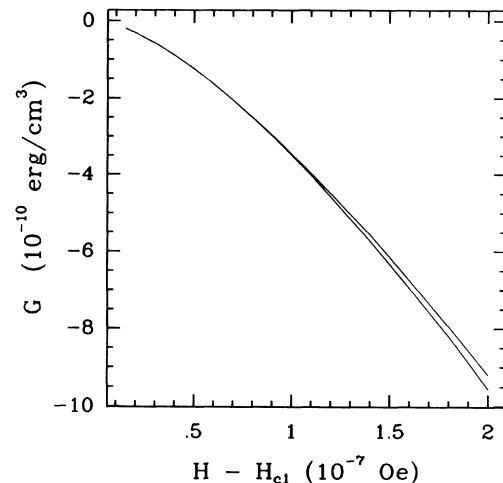


FIG. 1. The ground-state energy of the flux boson at $T=10.58$ K vs the external field. The upper curve is obtained with the "fluid" trial wave function and the lower curve with the "solid" trial wave function. The phase transition between these two states occurs at $H - H_{c1} = 0.71 \times 10^{-7}$ Oe when the Gibbs free energies are equal.

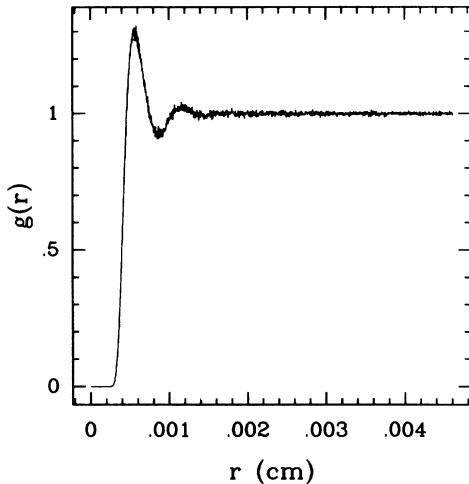


FIG. 2. The pair-correlation function of liquid state at the transition point $H - H_{c1} = 0.71 \times 10^{-7}$ Oe and $T = 10.58$ K.

the transition point, while the pair-correlation function $g(r)$, shown in Fig. 2, exhibits only a short-range order in the liquid right before freezing. The Lindemann ratios γ for the crystalline state are given in Table I for several external fields of interest at $T = 10.58$ K. The lattice melts at $T = 10.58$ K for γ larger than 0.282. For $T = 35$ K this value is 0.287, while for $T = 68$ K the Lindemann ratio at the melting line is 0.294. These values of γ_{melting} are consistent with $\gamma_{\text{melting}} = 0.3 \pm 0.02$ found in other quantum systems.¹⁸

The melting curve in the H - T diagram is depicted in Fig. 3. The circles denote our calculations and the solid line is the least-squares fit (for low T) by the formula $H_x - H_{c1} = \alpha T^2$. The best fit is obtained for $\alpha = 8.02 \times 10^{-10}$ Oe/K². The agreement with Eq. (1) is very good indicating the validity of the picture proposed by Nelson. The width of the entangled liquid phase is found to be quite narrow. However, it rises faster than T^2 at higher temperatures, as seen from Fig. 3, and eventually crosses over to the high-field melting curve: There, a qualitatively similar quantum interaction model can be constructed to describe a melting transition.¹⁹ We attribute this faster increase to the renormalization of H_{c1} downward from its mean-field value.²

For conventional isotropic type-II superconductors,

TABLE I. The Lindemann ratio γ in the crystalline state for several values of the external field at $T = 10.58$ K.

$H - H_{c1}$ (10^{-7} Oe)	γ
0.71	0.282
0.80	0.277
0.90	0.272
1.00	0.266
1.20	0.239
1.40	0.236

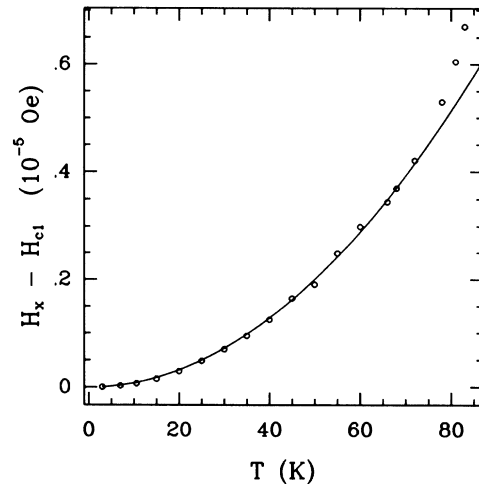


FIG. 3. The phase diagram for flux-lattice melting near the H_{c1} line in Y-Ba-Cu-O system. The circles are values obtained by the Monte Carlo calculation while the solid line represents a least-squares fit discussed in the text.

$M_z/M \approx 1$, $\kappa \approx 1$, and $T_c \approx 10$ K. From our calculations for the Y-Ba-Cu-O compound and the quantum correspondence theorem²⁰ we estimate that, except very close to $T_c(H=0)$, the melting field H_x and the corresponding transition densities in conventional superconductors would be several orders of magnitude smaller than in Y-Ba-Cu-O at a moderate temperature, say, 30 K. It is therefore of little interest to investigate the flux-liquid state in conventional superconductors. It is important to emphasize here that the appearance of the entangled flux-liquid phase in high- T_c superconductors is mainly caused by high critical temperatures and large mass anisotropy. The logarithmic dependence of the "mass" of a flux boson on the value of the Ginzburg-Landau parameter implies κ plays a less important role in flux melting close to the H_{c1} line. This is different from the flux melting in the region of the H_{c2} line, where the melting curves are suppressed well below the mean-field upper critical field line mainly due to the large value of κ .⁵ Finally, our results for $H_x(T)$ should be somewhat modified to account for a finite sample size and the fact that the mass of a flux boson is mostly of the magnetic origin in a very dilute case.²

In conclusion, we have observed the existence of a flux-liquid phase in high- T_c superconductors in the close vicinity of H_{c1} in a Monte Carlo simulation, and established the melting curve for the Y-Ba-Cu-O compound in this region of phase diagram. The large mass anisotropies and high critical temperatures in high- T_c oxides played key roles in the flux melting. We expect the melting tendency would be more pronounced in Bi-Sr-Ca-Cu-O materials in light of their much higher value of M_z/M . While we have concentrated here on the narrow region of the phase diagram in the vicinity of H_{c1} , where mapping to the quantum problem is best understood, we

expect that the region close to H_{c2} could also be investigated by similar methods, i.e., by defining a suitable effective quantum problem.

We would like to thank M. Robbins, C. E. Campbell, A. Singh, J. Belak, and particularly D. R. Nelson for useful discussions. This work was supported in part by the David and Lucile Packard Foundation.

¹L. Gammel, D. J. Bishop, G. J. Dolan, J. R. Kwo, C. A. Murray, L. F. Schneemeyer, and J. V. Waszczak, *Phys. Rev. Lett.* **59**, 2592 (1987); L. Gammel, L. F. Schneemeyer, J. V. Waszczak, and D. J. Bishop, *Phys. Rev. Lett.* **61**, 1666 (1988); E. H. Brandt, P. Esquinazi, and G. Weiss, *Phys. Rev. Lett.* **62**, 2330 (1989); R. N. Kleiman, P. L. Gammel, L. F. Schneemeyer, J. V. Waszczak, and D. J. Bishop, *Phys. Rev. Lett.* **62**, 2331 (1989).

²D. R. Nelson, *Phys. Rev. Lett.* **60**, 1973 (1988); D. R. Nelson and H. S. Seung, *Phys. Rev. B* **39**, 9153 (1989); D. R. Nelson, *J. Stat. Phys.* **57**, 511 (1989).

³M. A. Moore, *Phys. Rev. B* **39**, 136 (1989).

⁴M. P. Fisher, *Phys. Rev. Lett.* **62**, 1415 (1989).

⁵A. Houghton, H. A. Pelcovits, and A. Sudbø, *Phys. Rev. B* **40**, 6763 (1989).

⁶D. S. Fisher, *Phys. Rev. B* **22**, 1190 (1980); P. L. Gammel, A. F. Hebard, and D. J. Bishop, *Phys. Rev. Lett.* **60**, 144 (1988).

⁷T. K. Worthington, F. H. Holtzberg, and C. A. Feild (to be published); IBM report (to be published).

⁸M. C. Marchetti and D. R. Nelson, *Phys. Rev. B* **41**, 1910 (1990).

⁹For a discussion of these effects, see E. H. Brandt, *Phys. Rev. B* **34**, 6514 (1986); *Phys. Rev. Lett.* **63**, 1106 (1989).

¹⁰M. Schick, *Phys. Rev. A* **3**, 1067 (1971).

¹¹There is considerably more uncertainty in choosing the functional form of the Jastrow function in our case than in the helium problem due to the logarithmic nature of $K_0(x)$ for $x \ll 1$. We have tried other forms for $f(r)$ in Eq. (3), particularly the one involving $K_0(r/\lambda)$ in the exponential: The choice $a_2=3$ in Eq. (3) consistently gives the lowest energy in the functional space explored.

¹²J. P. Hansen and E. L. Pollock, *Phys. Rev. A* **5**, 2651 (1972).

¹³D. Ceperley, G. V. Chester, and M. H. Kalos, *Phys. Rev. B* **17**, 1070 (1978).

¹⁴L. Krusin-Elbaum, R. L. Greene, F. Holtzberg, A. P. Malozemoff, and Y. Yeshurun, *Phys. Rev. Lett.* **62**, 217 (1989); A. F. Hebard, A. T. Fiory, and D. R. Harshman, *Phys. Rev. Lett.* **62**, 2885 (1989); R. L. Greene, L. Krusin-Elbaum, and A. P. Malozemoff, *Phys. Rev. Lett.* **62**, 2886 (1989).

¹⁵M. Metropolis, A. W. Rosenbluth, H. N. Rosenbluth, A. M. Teller, and E. Teller, *J. Chem. Phys.* **21**, 1087 (1953).

¹⁶W. L. McMillan, *Phys. Rev.* **138**, A442 (1965).

¹⁷D. Schiff and L. Verlet, *Phys. Rev.* **160**, 293 (1960).

¹⁸D. Ceperley, *Phys. Rev. B* **18**, 3126 (1978); S. T. Chui (to be published). While all Monte Carlo studies known to us indicate the existence of a 2D quantum solid at $T=0$ for γ less than this "magic" value, one may be concerned that the neglect of a proper symmetrization of the Nosanow wave function ignores the coherent ring exchanges which could be detrimental to the positional long-range order. Recent studies using the "shadow" wave function, which does have the required symmetry, do confirm the stability of a solid—furthermore, the symmetrization is found not to result in significant differences from the Nosanow case; S. Vitiello (private communication).

¹⁹Lei Xing and Zlatko Tešanović (unpublished); D. R. Nelson (private communication).

²⁰See, for example, L. H. Nosanow, L. J. Parish, and F. J. Pinski, *Phys. Rev. B* **11**, 191 (1975), and references therein.